

Analytical and Experimental Comparison of Composite Laminate Elastic Properties

Amir Baharvand

Contents

2	Introduction	1
3	Burn off Analysis	2
4	Elastic Properties	3
4.1	Rule of Mixture	3
4.2	10%-Rule	4
4.3	Classical Laminate Theory (CLT)	5
5	Discussion	5
6	Laminate Factor of Safety	7
6.1	Maximum Strain and Maximum Stress	8
6.2	Tsai-Hill	8
6.3	Hashin	9
7	Conclusion	10

2 Introduction

Elastic properties play a critical role in defining the stress-strain relation or the so-called constitutive law. Accuracy in determining the elastic properties helps researchers predict the material behavior under different loading conditions. This report aims to provide a comparison between the elastic properties determined from the classical laminate theory and tensile testing. The test coupons are manufactured using the autoclave and vacuum infusion. The rule of mixture and the 10%-rule are further invoked to compare with the CLT and experiment. Eventually, the first-ply failure is utilized to predict the factor of safety of the composite laminates.

This report is divided into the following sections. Section. 3 discusses the determination of fiber volume fraction. Section. 4 summarizes the calculation of the elastic properties from different methods. A discussion on the result and

the difference in laminate quality using the autoclave and vacuum infusion are given in Section. 5. Finally, Section. 6 reviews calculation of the factor of safety.

3 Burn off Analysis

Table. 1 and Table. 2 list the mechanical properties of the fiber (AS-4 Carbon) and resin (Epoxy 3501-6) used in this study. The laminate stacking sequence is $[\pm 45/0/90/0]_s$.

Property	Symbol	Unit	Value
Density	ρ_f	kg/cm ³	1.81
Longitudinal modulus	E_{1f}	GPa	235
Transverse modulus	E_{2f}	GPa	15
Shear modulus	G_{12f}	GPa	27
Poisson's ratio	ν_{12f}	-	0.20

Table 1: AS-4 Carbon mechanical properties

Property	Symbol	Unit	Value
Density	ρ_m	kg/cm ³	1.27
Young's modulus	E_m	GPa	4.3
Shear modulus	G_m	GPa	1.6
Poisson's ratio	ν_m	-	0.35

Table 2: Epoxy 3501-6 mechanical properties

The burn off test was conducted according to ASTM D3171-22 [1], method 1 procedure G. The crucible mass is 15 g and the void content is assumed to be zero. The autoclave and vacuum infusion laminate density are 1.60g/cm³ and 1.45g/cm³, respectively. First, the mass of the dry fiber, m_f , (after burn off) is calculated by deducting the crucible mass from the mass post-burn off. Then, fiber weight fraction, W_f , and fiber volume fraction, V_f are calculated according to Eq. 1 and Eq. 2.

$$W_m = \frac{m_f}{m_i} \times 100 \quad (1)$$

$$V_f = \frac{m_f}{m_i} \frac{\rho_i}{\rho_f} \times 100 \quad (2)$$

where m_i and ρ_i are the composite mass (before burn off) and density and ρ_f is the fiber density. Next, the resin weight fraction, W_m , and volume fraction, V_m are calculated from Eq. 3 and Eq. 4.

$$W_m = \frac{m_i - m_f}{m_i} \times 100 \quad (3)$$

$$V_m = 100 - V_f \quad (4)$$

where ρ_m is the resin density.

Table. 3 and Table. 4 summarize the fiber/resin volume fraction along with their mean and standard deviation (STD). The mean values of the fiber volume fraction are used in Section. 4 to calculate the elastic properties. The small value of STD indicates the high precision of the burn off test. Further discussion on the accuracy of the test result is given in Section. 4.

Table 3: The autoclave laminate fiber/resin volume fraction.

Specimen	Post-Burnoff mass (crucible+contents) [g]	Crucible mass [g]	m_f [m]	m_c [m]	W_f [%]	V_f [%]	W_m [%]	V_m [%]
1	80.0	15.0	65.0	94.0	69.1489	61.1261	30.8511	38.8739
2	74.0	15.0	59.0	85.3	69.4118	61.3585	30.5882	38.6415
3	76.0	15.0	61.0	88.2	69.3182	61.2757	30.6818	38.7243
					Mean	61.25		38.75
					STD	0.12		0.12

Table 4: The vacuum infusion laminate fiber/resin volume fraction.

Specimen	Post-Burnoff mass (crucible+contents) [g]	Crucible mass [g]	m_f [m]	m_c [m]	W_f [%]	V_f [%]	W_m [%]	V_m [%]
1	89.0	15.0	74.0	172.0	43.0233	34.4661	56.9767	65.5339
2	84.0	15.0	69.0	166.0	41.5663	33.2989	58.4337	66.7011
3	78.0	15.0	63.0	154.0	40.9091	32.7725	59.0909	67.2275
					Mean	33.51		66.49
					STD	0.87		0.87

4 Elastic Properties

4.1 Rule of Mixture

The rule of mixture (ROM) assumes unidirectional fibers for the determination of lamina properties; however, in case of a laminate with different fiber angles, the ROM is incapable of yielding correct values. This is due to the lack of contribution of each ply to a certain property. For instance, the contribution from $\pm\theta$ and 90° is not the same as 0° plies in axial loading. The contribution of each ply can be determined using the so-called Krenchel orientation efficiency factor, η_θ [2] and is defined according to Eq. 5.

$$\eta_\theta = \sum a_n \cos^4(\theta_n) \quad (5)$$

where a_n is the fraction of layers with orientation angle θ_n with respect to the loading direction. Rewriting the ROM using Krenchel orientation efficiency factor gives

$$\begin{aligned} E_x &= \eta_{\theta 1} E_f V_f + E_m (1 - V_f) \\ E_y &= \eta_{\theta 2} E_f V_f + E_m (1 - V_f) \end{aligned} \quad (6)$$

in which E_x and E_y are the laminate longitudinal and transverse elastic modulus. η_{θ} values are tabulated in Table. 5. It can be seen that the contribution of 90° to the longitudinal elastic modulus is zero. Similarly, 0° plies have no effect on the transverse elastic modulus.

	a_n			$\cos^4(\theta)$			$\eta_{\theta 1}$	$\eta_{\theta 2}$
	0°	90°	$\pm 45^\circ$	0°	90°	$\pm 45^\circ$		
x -direction	0.4	0.2	0.4	1	0	0.25	0.5	-
y -direction	0.4	0.2	0.4	0	1	0.25	-	0.3

Table 5: η_{θ} values for determination of the longitudinal and transverse elastic modulus using the ROM.

4.2 10%-Rule

The 10%-rule [3] provides a quick and reliable initial estimation of elastic properties in composite laminates and is popular in the aerospace industry where most of the laminate include 0° , 90° and $\pm 45^\circ$. According to this rule, the contribution of the $\pm 45^\circ$ and 90° plies to the overall laminate elastic modulus is one-tenth of a 0° ply in axial loading. Similarly, 0° and 90° plies contribute one-tenth of an equivalent $\pm 45^\circ$ ply to the in-plane shear modulus. Therefore, the 10%-rule can be summarized as

$$\begin{aligned} E_x &= E_{11}(0.1 + 0.9\lambda_0) \\ E_y &= E_{11}(0.1 + 0.9\lambda_{90}) \\ \mu_{xy} &= G_{12}(0.025 + 0.234\lambda_{\pm 45}) \end{aligned} \quad (7)$$

where

$$\begin{aligned} E_{11} &= E_f V_f + E_m (1 - V_f) \\ \frac{1}{G_{12}} &= \frac{V_f}{G_f} + \frac{(1 - V_f)}{G_m} \end{aligned}$$

E_{11} is the longitudinal modulus, G_{12} and μ_{xy} are the fiber and laminate in-plane shear modulus, λ_0 , λ_{90} and $\lambda_{\pm 45}$ denote the fraction of 0° , 90° and $\pm 45^\circ$ plies. For the given stacking sequence, $\lambda_0 = 0.4$, $\lambda_{90} = 0.2$ and $\lambda_{\pm 45} = 0.4$.

4.3 Classical Laminate Theory (CLT)

Figure. 1 summarizes the approach utilized by the CLT. The left column is known as the ABD matrix, which connects the applied force/moment to strain/curvature. The right column solves for the global strain/curvature of the laminate using the ABD matrix and the applied force/moment. Global stress is determined using the constitutive law (stress-strain relation) and the strain and stress of each ply are calculated using the transformation of their corresponding global values.

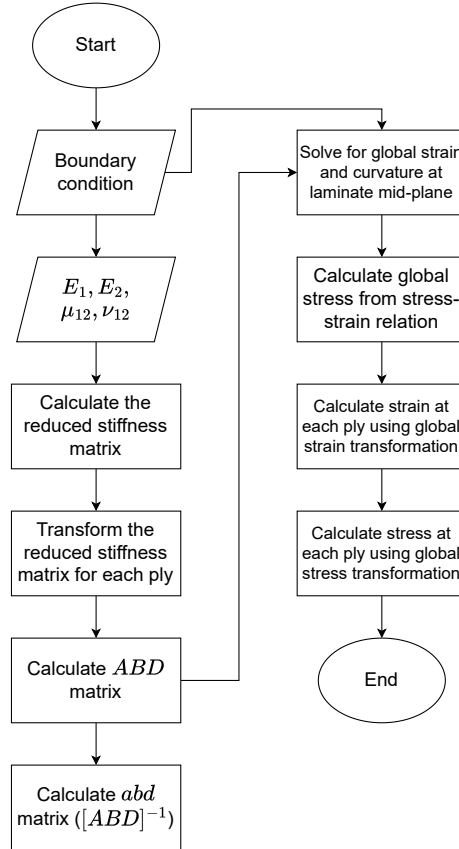


Figure 1: The composite laminate theory (CLT) flowchart.

5 Discussion

As expected, the result from Section. 3 shows a higher fiber volume fraction for the autoclave laminate. The process from vacuum bagging to curing in an autoclave is performed inside a pressurized vessel under controlled temperature and

pressure. The pressurized vessel increases the compaction between the vacuum bag and fibers, leading to minimum void and high fiber content. In contrast, the vacuum infusion uses atmospheric pressure for compaction, leading to a higher void content and lower fiber volume fraction in comparison to the autoclave. Furthermore, in vacuum infusion, the curing is usually performed at room temperature or after infusion, in an oven which complicates the curing parameters. As a result, the mechanical properties of a laminate manufactured using the vacuum infusion are inferior to the autoclave.

Table. 6 and Table. 7 list the elastic properties of the autoclave and vacuum infusion laminates using different methods. A noticeable difference in the longitudinal elastic modulus of the autoclave laminate between the analytical and experimental results is visible. Despite the high volume fraction of the autoclave laminate (61.25%), there is a noticeable difference of 18.4% between the measured E_x and the CLT result. Several reasons might have caused this discrepancy. The misalignment in the tensile testing machine results in an underestimated value of E_x . Another reason could be the presence of delamination in the testing coupon due to improper manufacturing. Hence, inspection using the non-destructive testing method, *i.e.*, C-scan of the manufactured laminates for detecting defects like delamination, is recommended [4]. Furthermore, the fiber and resin volume fraction from Table. 3 shows high fiber content in the autoclave laminate which contradicts the experimental results of E_x . This contradiction concludes the presence of local delamination in the autoclave laminate, being more pronounced in the region where the tensile testing coupons are cut. While the ROM and CLT can predict the transverse elastic modulus, E_y , the 10%-rule gives a lower value. The difference between the analytical and experimental values for the shear modulus and Poisson's ratio is negligible, which shows the advantage of the 10%-rule in predicting the shear modulus and Poisson's ratio of the multi-axial laminate with less computational effort than the CLT.

Elastic properties	Symbol	Unit	ROM	10%-rule	CLT	Experiment	COV [%]
Longitudinal elastic modulus	E_x	GPa	73.635(20.3)	66.978(9.4)	72.436(18.4)	61.2 $^{61.9}_{60.5}$	1.2
Transverse elastic modulus	E_y	GPa	44.848(-1.4)	40.769(-10.4)	46.473(2.1)	45.5 $^{47.5}_{43.5}$	4.3
In-plane shear modulus	μ_{xy}	GPa	-	17.293(0)	17.238(0)	16.8 $^{17.8}_{15.8}$	6.1
In-plane Poisson's ratio	ν_{xy}	-	-	-	0.3118(0)	0.31 $^{0.32}_{0.30}$	2.4

Table 6: Comparison of the autoclave laminate elastic properties using different methods (numbers in parentheses indicate the relative difference with the experiment)

The analytical results from the vacuum infusion show a good agreement with the experiment. The maximum difference is 13.8% for the transverse elastic modulus using the 10%-rule. This implies a uniform distribution of fibers

through the laminate and good manufacturing quality.

Elastic properties	Symbol	Unit	ROM	10%-rule	CLT	Experiment	COV [%]
Longitudinal elastic modulus	E_x	GPa	48.165(5.6)	37.539(-6.2)	41.084(2.7)	40 ^{41.8} _{38.2}	4.5
Transverse elastic modulus	E_y	GPa	29.953(-0.1)	22.850(-13.8)	26.822(1.2)	26.5 ^{28.5} _{24.5}	7.4
In-plane shear modulus	μ_{xy}	GPa	-	10.700(0)	9.835(0)	9.82 ^{10.63} _{9.01}	8.2
In-plane Poisson's ratio	ν_{xy}	-	-	-	0.3205(0)	0.31 ^{0.32} _{0.30}	3.1

Table 7: Comparison of the infused laminate elastic properties using different methods (numbers in parentheses indicate the relative difference with the experiment).

The predicted and measured elastic properties are plotted in Figure. 2. The result shows the conservative nature of the 10%-rule in comparison to the ROM and CLT and the application of the 10%-rule for a quick estimation of the elastic properties of the multi-axial laminates.

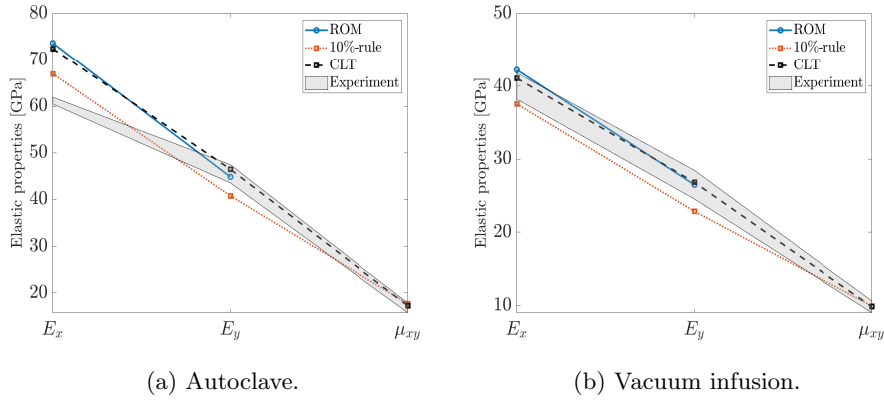


Figure 2: Analytical and experimental elastic properties comparison.

6 Laminate Factor of Safety

The methodology for determination of the factor of safety (S.F) in the present report is based on the failure index (F.I) in the first ply failure. Table. 8 lists the strength values of the autoclave and vacuum infusion laminates. It is worth noting that the worst-case scenario (lower bound of the strength values) is used for calculating the factor of safety for each laminate. The applied stress is integrated through the laminate thickness to convert them into stress resultant.

Property	Symbol	Unit	Autoclave		Vacuum infusion	
			Value	COV[%]	Value	COV[%]
Longitudinal tensile strength	X_t	MPa	2200	1.2	2050	3.7
Longitudinal compressive strength	Y_c	MPa	2350	16	2300	23
Transverse tensile strength	Y_t	MPa	50	2.8	42	6.1
Transverse tensile strength	Y_c	MPa	56	17	51	25
In-plane shear strength	S	MPa	72	7.6	68	12

Table 8: Strength values of the autoclave and vacuum infusion laminates in different directions.

6.1 Maximum Strain and Maximum Stress

According to the maximum strain theory, failure occurs when the strain at one ply exceeds the ultimate strain. The failure index for this theory is

$$F.I = \max\{\text{abs}\{\frac{\epsilon_{11}}{eX_t}, \frac{\epsilon_{11}}{eX_c}, \frac{\epsilon_{22}}{eY_t}, \frac{\epsilon_{22}}{eY_c}, \frac{\epsilon_{12}}{eS}\}\} \quad (8)$$

where eX , eY and eS are the ultimate longitudinal, transverse and in-plane strain, subscripts t and c indicate the tension and compression, 1, 2 and 3 designate the ply coordinate system, ϵ is the strain and "max" and "abs" are the maximum and absolute. Similarly, for the maximum stress theory, failure happens when the stress in a ply reaches the ultimate strength; hence, the failure index for the maximum stress can be defined as

$$F.I = \max\{\text{abs}\{\frac{\sigma_{11}}{X_t}, \frac{\sigma_{11}}{X_c}, \frac{\sigma_{22}}{Y_t}, \frac{\sigma_{22}}{Y_c}, \frac{\sigma_{12}}{S}\}\} \quad (9)$$

where X , Y and S are the ply ultimate longitudinal, transverse and in-plane strength and σ is the local stress. Hence, the factor of safety for the maximum strain and maximum stress failure criteria is [5]

$$S.F = \min\{\frac{1}{F.I}\} \quad (10)$$

Please see ?? for a comment on the result from maximum strain theory.

6.2 Tsai-Hill

According to Tsai-Hill failure criterion, failure occurs when

$$F.I = \frac{\sigma_{11}^2}{X^2} + \frac{\sigma_{22}^2}{Y^2} - \frac{\sigma_{11}\sigma_{22}}{X^2} + \frac{\sigma_{12}^2}{S^2} \geq 1 \quad (11)$$

where X and Y are the tensile/compressive strength and change signs accordingly, *i.e.* in case of compressive stress, X and Y become X_c and Y_c . Hence, the factor of safety becomes [5]

$$S.F = \sqrt{\frac{1}{\frac{\sigma_{11}^2}{X^2} + \frac{\sigma_{22}^2}{Y^2} - \frac{\sigma_{11}\sigma_{22}}{X^2} + \frac{\sigma_{12}^2}{S^2}}} \quad (12)$$

6.3 Hashin

The implemented Hashin excludes the coupling between the normal and in-plane shear stress [6]. Hashin failure criterion differentiates between the fiber and matrix failure; therefore, two failure indices are defined according to Eq. 13.

$$\begin{aligned} (\text{F.I})_f &= \frac{\sigma_{11}^2}{X^2} \geq 1 \\ (\text{F.I})_m &= \frac{\sigma_{22}^2}{Y^2} + \frac{\sigma_{12}^2}{S^2} \geq 1 \end{aligned} \quad (13)$$

where the former is for the fiber and the latter is for the matrix failure. Similar to Tsai-Hill, the factors of safety for the fiber and matrix become

$$\begin{aligned} (\text{S.F})_f &= \sqrt{\frac{1}{(\text{F.I})_f}} \\ (\text{S.F})_m &= \sqrt{\frac{1}{(\text{F.I})_m}} \end{aligned}$$

The final factor of safety is the minimum of $(\text{S.F})_f$ and $(\text{S.F})_m$.

$$\text{S.F} = \min\{(\text{S.F})_f, (\text{S.F})_m\} \quad (14)$$

The factor of safety for five different load cases is presented in Table. 9 and Table. 10. Figure. 3 illustrates different failure criteria in this report. The maximum strain theory gives lower values of the factor of safety compared to the other. This difference is more pronounced in load case #5. In this load case, both Hashin and maximum stress theories yield a similar result as the coupling between the shear and longitudinal stress, σ_{11} , is neglected in Hashin failure criterion [6].

Case #	Description	Magnitude [MPa]	Maximum strain	Maximum stress	Tsai-Hill	Hashin
1	Longitudinal tension	80	5.51	5.97	6.16	6.24
2	Longitudinal compression	-65	6.78	7.35	7.28	7.35
3	Transverse tension	5	56.57	59.44	61.82	62.16
4	Transverse compression	-5	56.57	59.44	59.20	59.44
5	In-plane shear	20	10.49	14.93	12.43	14.09

Table 9: Factor of safety of each load case for the autoclave laminate.

Case #	Description	Magnitude [MPa]	Maximum strain	Maximum stress	Tsai-Hill	Hashin
1	Longitudinal tension	80	3.47	3.82	3.91	3.94
2	Longitudinal compression	-65	4.28	4.70	4.68	4.70
3	Transverse tension	5	36.31	38.50	39.59	39.70
4	Transverse compression	-5	36.31	38.50	38.42	38.50
5	In-plane shear	20	6.66	9.44	8.77	9.45

Table 10: Factor of safety of each load case for the vacuum infusion laminate.

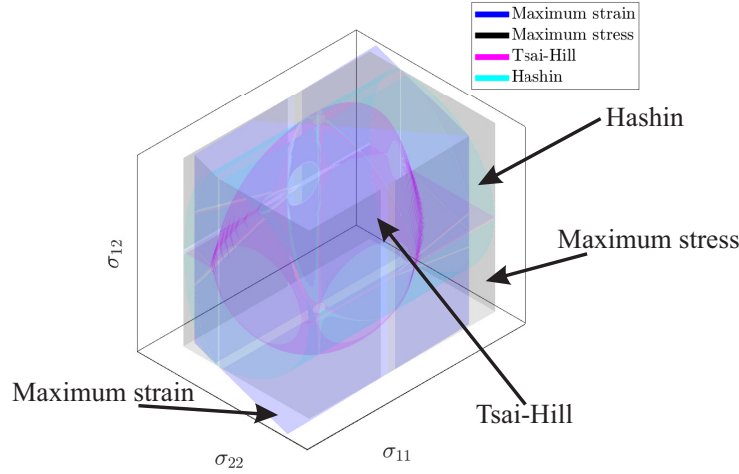


Figure 3: An schematic representation of the failure criteria.

7 Conclusion

A comparative study between analytical and experimental values of the elastic properties of two laminates manufactured using the autoclave and vacuum infusion is presented. The laminate manufactured using the autoclave shows superior mechanical properties compared to the vacuum infusion laminate. The autoclave's elastic properties and fiber volume fraction show almost a twofold increase, which justifies the application of this manufacturing method to the aerospace industry, where both strength and stiffness are important. The result shows a good agreement between the experiment and composite laminate theory. The 10%-rule leads to a more conservative result compared to the rule of mixture and classical laminate theory.

References

- [1] ASTM International, “ASTM D3171: Standard Test Methods for Constituent Content of Composite Materials,” vol. 15.03, 2022.
- [2] H. Krenchel, “Fibre reinforcement; theoretical and practical investigations of the elasticity and strength of fibre-reinforced materials,” 1964.
- [3] Hart-Smith and L. J., “The ten-percent rule for preliminary sizing of fibrous composite structures,” *WeiEn*, vol. 52, pp. 29–45, 1992.
- [4] K. Imielińska, M. Castaings, R. Wojtyra, J. Haras, E. L. Clezio, and B. Hosten, “Air-coupled ultrasonic c-scan technique in impact response testing of carbon fibre and hybrid: glass, carbon and kevlar/epoxy composites,” *Journal of Materials Processing Technology*, vol. 157-158, pp. 513–522, 12 2004.
- [5] Autodesk, *Helius Composite Support and Learning*. United States: Autodesk, 2016.
- [6] Z. Hashin and A. Rotem, “A fatigue failure criterion for fiber reinforced materials,” *Journal of Composite Materials*, vol. 7, pp. 448–464, 7 2016.